Journal of Marine Systems 77 (2009) 418–427

Contents lists available at ScienceDirect

Journal of Marine Systems

journal homepage: www.elsevier.com/locate/jmarsys

Using high sampling-rate ADCP for observing vigorous processes above sloping [deep] ocean bottoms

Hans van Haren

Royal Netherlands Institute for Sea Research (NIOZ), P.O. Box 59, 1790 AB Den Burg, The Netherlands

ARTICLE INFO

Article history:
Received 24 September 2007
Accepted 29 October 2008
Available online 11 November 2008

Keywords:
High-resolution ADCP observations
Upslope propagating fronts and boluses
Bore turbulence
Continental slopes

ABSTRACT

Above sloping bottoms in the ocean mixing processes are not predominantly generated by shear-induced turbulence via bottom friction. Instead, the restratifying buoyancy forces and internal waves create a highly non-linearly varying environment including 'stratified turbulence'. Most of the resulting vigorous mixing processes that dominate sediment resuspension occur during the passage of frontal bores or solitary boluses, 'solibores'. Here, the observed evolution of different forms of highly non-linear strictly upslope moving 'waves', bores or boluses are reviewed from various NIOZ projects at deep sloping bottom sites ranging from 500 to 3000 m.

Such fronts pass a fixed site within a few minutes, extending some 60 ± 30 m above the bottom and occurring over much larger periods at once per subinertial or meso-scale period or approximately, but not exactly, once per tidal harmonic period. In order to observe the details of such solibore one needs specific, high-sampling rate equipment. A suitable piece of equipment is a bottom-mounted 4-beam 300 kHz acoustic Doppler current profiler (ADCP), provided it samples at a rate of about once per second over a period of at least several weeks. Not just the three components of current velocity [*u*,*v*,*w*] are monitored over a range of some 80 m at 1 m intervals, but also the relative 'echo intensity' dI, which is a measure for suspended matter and stratified turbulence. Such ADCP-observations are combined and compared with high-resolution temperature measurements. Fine details show a turbulent inner core with more or less laminar streamlines outside it. Whether a front or a bolus, the bore is never observed as a completely closed contour, as swept up turbulent material is sucked into the core at the rear end.

1. Introduction

Diapycnal mixing and transport are of eminent importance for the redistribution of material in seas and ocean and thereby determine the fate of a variety of processes like plankton growth, sediment resuspension and the maintenance of deep-ocean stratification. One of the key mechanisms to such interior mixing are thought to be internal waves. As linear, purely sinusoidal waves do not mix, they must transfer energy to non-linear, usually high-frequent, [breaking] waves before irreversible mixing can take place. Highly non-linear internal solitary waves or 'solibores', 'boluses' (henceforth 'SWB') demonstrate closed streamlines and thus can transport material (Wallace and Wilkinson, 1988). A major area for turbulent dissipation of non-linear waves generated in the interior is above topography. There, material transport by such waves is largely up a sloping bottom as opposed to more commonly known downslope gravity currents.

Here, we are concerned with the observational details of such 'transport' waves. In particular, we consider near-bottom motions directly affecting sediment resuspension above sloping topography. The problem of observations of these phenomena is that highly non-linear waves occur quite randomly in time, although in certain areas a quasi-tidal periodicity of interfacial solitary waves is noted (e.g., Inall et al., 2000). Due to their non-linearity, their passage is relatively quick with time, $O(1/N)$, where N represents the buoyancy frequency, having typical

E-mail address: hansvh@nioz.nl.

0924-7963/$ – see front matter © 2008 Elsevier B.V. All rights reserved.
doi:10.1016/j.jmarsys.2008.10.012

values of 10^{-2}–10^{-3} s^{-1}. The detailed observation of such waves and inherent energy-carrying turbulent scales requires instrumentation sampling at rates of 0.1–1 per second and resolving spatial vertical scales $\Delta z = O(1\ m)$ over vertical ranges O(100 m). This is possible with specific equipment, as has been known for some time (see high-frequency sample in LaFond, 1966).

Near-surface internal solitary waves are commonly modelled as waves of depression following KdV-theory, because the deeper layer is much larger than the surface homogeneous layer (e.g., Vlasenko and Hutter, 2002). Once generated, waves propagating onto a sloping bottom, that is 'shoaling' and "back" to the source of, e.g., internal tides, must at some point change from internal solitary waves of depression to waves of elevation. These two types of waves have been observed by LaFond (1966), but their transfer has only recently been evidenced using echosounder observations of echo amplitude, not [current] Doppler shift, above a continental shelf (Orr and Mignerey, 2003). Similar observations were used to visualize near-surface overturning (closed-contouring) of internal solitary waves (Moum et al., 2003). The ship-borne 100–200 kHz echosounders were sampled at a rate of about once per second, resolving ~1 m vertically across some 100 m.

Much of the information of shoaling internal waves and their propagation or run up a sloping bottom comes from laboratory experiments (e.g., Wallace and Wilkinson, 1988; Ivey and Nokes, 1989; Dauxois et al., 2004; Grue, 2004) and numerical modelling (e.g., Vlasenko and Hutter, 2002; Venayagamoorthy and Fringer, 2005). Two types of upslope propagating nonlinear motions emerge: 1) steep fronts, occasionally preceded by a very near-bottom surge, and normally followed by a core of turbulence and sometimes by a train of more or less regular waves, limited in number, 2) single boluses of closed contoured core of turbulence that tend to sweep water around them before 'sucking' it into the turbulent core at the trailing edge. The former are suggested to be generated via either near-critical internal wave breaking or shoaling internal solitary waves while the latter seem more likely to follow from regular [internal wave] depression of the large-scale stratification (Fig. 1).

Following rare observations at sea of near-bottom boluses using rapid XBT-observations up an Australian shelf (Wallace and Wilkinson, 1988), some recent evidence from shipborne observations demonstrated the propagation of waves of elevation up a sloping continental shelf in ~100 m water depth, including large vertical currents and enhanced echo intensity, a measure for sediment resuspension (Klymak and Moum, 2003). Using moored instrumentation sampling once per 30 s Hosegood et al. (2004) showed the upslope propagation of steep fronts associated with solibores. In conjunction with slower sampled optical backscatter and sediment trap data they proved that short, O(10 min), duration solibore dominated the sediment resuspension and upslope transport averaged over 4 days. In contrast, they found that the solibores' contribution to tidally averaged eddy diffusivity amounted about 30–50% of the canonical value of 10^{-4} m^2 s^{-1} required to maintain the deep-ocean stratified, despite the short-term value of $O(10^{-2}$ m^2 $s^{-1})$ during the bore's passage. Waves of elevation are found more effective for sediment resuspension than waves of depression.

Here we present new observational material of solibores and boluses affecting sediment resuspension after reviewing some previous moored SWB-observations using off-the-shelf acoustic Doppler current profiler (ADCP) and NIOZ-built instrumentation.

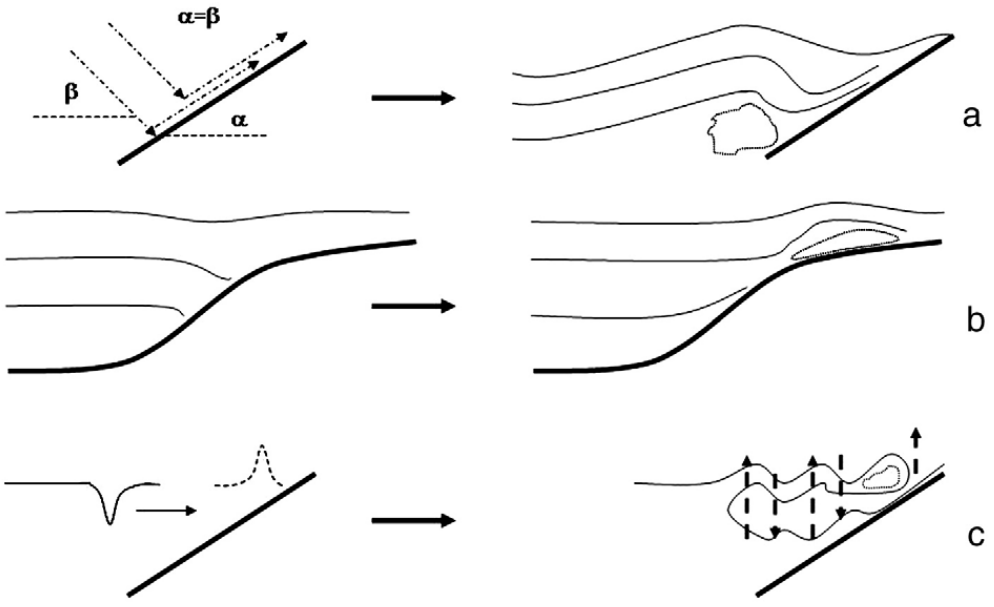

Fig. 1. Impression of several possible mechanisms leading to steep upslope propagating fronts, bores or boluses. In all panels thin solid lines represent isopycnals, dotted lines turbulent cores. In the left column the interior process is depicted that is going to interact with the slope, in the right column the resulting near-bottom upslope propagating phenomenon. a. Near-critical reflection of internal wave beams (dash–dot arrows) for which angle β to the vertical matches bottom slope angle α, after Ivey and Nokes (1989), Dauxois et al. (2004), b. isopycnal depression and generation of boluses during the elevation phase, after Wallace and Wilkinson (1988), Venayagamoorthy and Fringer (2005), and c. internal solitary wave of depression shoaling, first becoming internal wave of elevation (dashed isopycnal) before becoming a bore (or 'bolus') with large vertical motions extending up to the surface (heavy arrows), after Vlasenko and Hutter (2002).

2. A review of [one decade of] moored ADCP observations on SWB

2.1. Methodology

The data to be discussed in this paper are all from an RDI four-beam, broadband ADCP, mostly mounted in a bottom landing frame. To the center of the frame a 60–100 m line is attached, which holds different, mainly NIOZ-built, thermistor strings below a sub-surface buoy (Fig. 2). Over time, two frames have been used, but the upward looking ADCP has been always some 1.7 m above the bottom. Initially, a 600 kHz ADCP has been used (maximum 50 m range, 100 MB memory). From 2002 onwards, a 300 kHz ADCP is used (~80 m range, 500 MB memory, in 2005 extended to 2 GB). The ADCPs are set to resolve 0.5 or 1 m vertical intervals, which is the resolution of the thermistor strings, but the actual vertical resolution given by the 'transmission length' is 1.7 and 3.1 m, respectively.

With the extent of the memories the sampling rate became faster. For a sampling period of 15 days it ranged from 30 s (1999) via 15 s (2002) to 0.5–2 s (2005). The NIOZ-1 thermistor string (32 sensors, 0.04 mK relative accuracy) could sample at once per 20 s over 15 days, while NIOZ-2 (128 sensors, 1 mK relative accuracy) at a rate of 1 Hz. The newly built NIOZ-3 (first trial in 2006; 101 independent sensors, <1 mK relative accuracy) can sample at 2 Hz during 1 year.

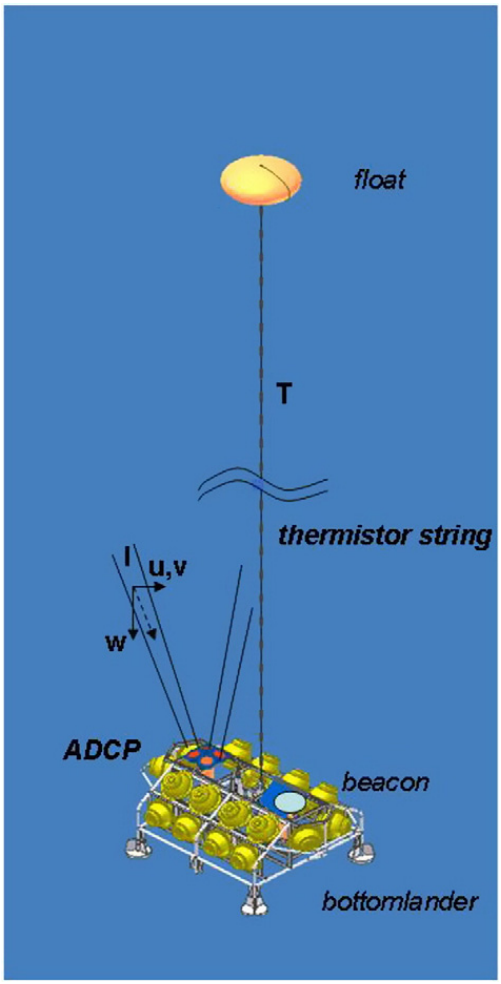

Fig. 2. Typical mooring set-up with bottom lander holding upward looking ADCP and thermistor string under single float. The release mechanism causes the thermistor string and lander to surface separately.

Five variables are extracted from the ADCPs per depth level: current components u (cross-slope), v (along-slope), w (either vertical or bottom-normal depending on the purpose of analysis), "error" velocity e, defined as the difference of the sum of opposing beam pair velocities and useful for verifying the quality or error of w and estimating the amount of current inhomogeneity over the beam spread, and relative echo intensity $dI = I - \langle I \rangle$, where I represents the measured acoustic backscatter and $\langle\rangle$ the time mean. This subtraction of the mean per depth level at least accounts for water attenuation of sound. It is used only to provide a relative measure for suspended matter concentration and turbulence. In principle the use of acoustic backscatter cross section would be better, as it varies linearly with suspended matter concentration rather than log-linearly, but we lack proper calibration here to employ an appropriate suspended sediment model like in Merckelbach (2006). The instrumental noise error in w (Δw) depends on the instrumental set-up. Here, typically $\Delta w = 2.5\text{–}7.5 \times 10^{-3}$ m s^{-1} per stored ensemble value.

The $\theta = 20°$ slant angle beams of the ADCP's average current estimates over horizontal distances between 2 and 55 m (for 3–80 m range), but the dI is measured within each of the four beams that only spread 1.5° (4 m horizontally at 80 m distance from the ADCP). For the internal waves under study, having periods of 1000 s (buoyancy period) or larger, even the averaging over the beam spread of ~30 m is adequate to resolve them. These waves have wavelengths O(100–1000 m). However, the ~1 Hz sampling will inadequately sample incoherent "eddy" structures, even when advected passed the beams at speeds up to 0.7 m s^{-1}. Therefore, w is always compared with the properly scaled e (van Haren et al., 1994) to demonstrate the amount of inhomogeneous motions.

So far, data collection has been concentrated above topography in the North-Atlantic Ocean, mainly above its continental slopes (Fig. 3). Topography varied from very smooth and gentle 1% slopes in the Faeroe–Shetland Channel, to very rugged, steep >10% and canyon-like slopes in the Bay of Biscay. Observational depths ranged from about 100 m to nearly 3000 m.

2.2. Overview of shallow and deep observations

Using 30-s sampled data during 2 weeks in 1999 above the Faeroe–Shetland Channel slope (FSC99) at ~500 m, Hosegood et al. (2004) demonstrated the dominance of upslope propagating solibores for sediment resuspension. They did so, after analyzing additional data from OBS-sensors and much slower sampled sediment traps. Although details of the turbulent cores were not revealed due to the 30-s sampling, it was clearly shown that steep fronts moved strictly up the slope, with upward motions that extended above the ADCP's range preceding the front and downward motions immediately thereafter, followed by train of 5–7 more or less regular waves. The occurrence of once per ~4 days suggested that the bores were mainly generated in response to atmospheric disturbances.

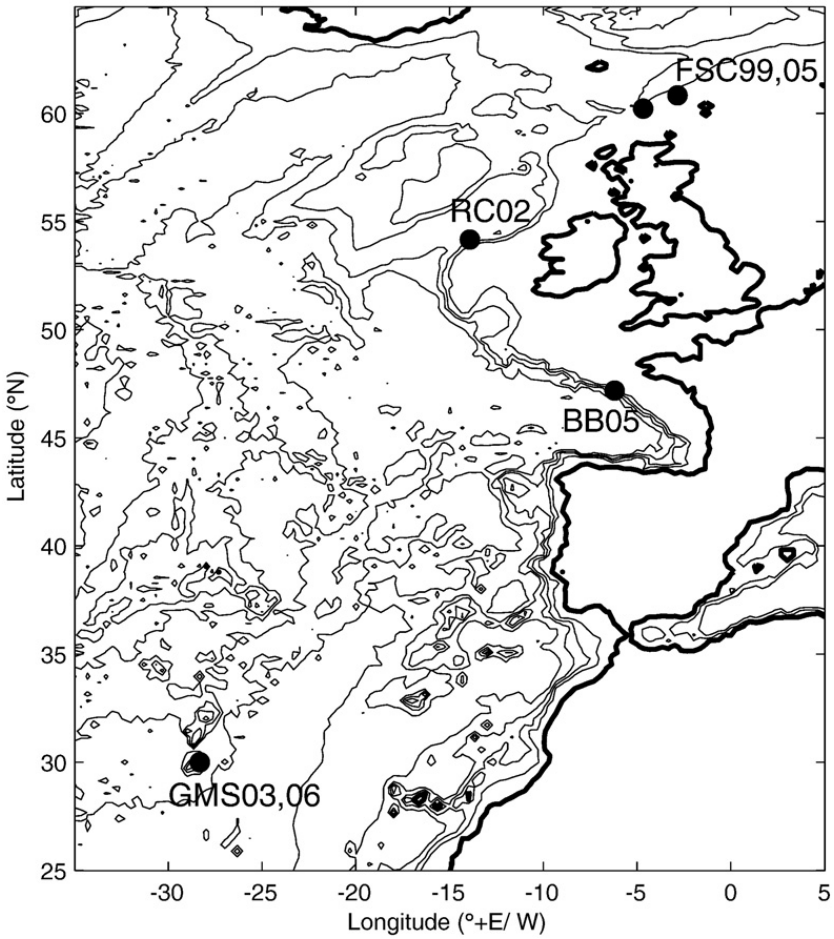

Fig. 3. Mooring positions (●) above topographic features in the North-East Atlantic Ocean. In the Faeroe–Shetland Channel (FSC) two 2–3 week campaigns were held, in 1999 (99) and 2005 (05). RC02 represents a 6-week campaign in the Rockall Channel in 2002, BB05 a 2.5 day campaign at ~1450 m in the Bay of Biscay and GMS03,06 two 2 week campaigns just below the summit of Great Meteor Seamount in 2003 and 2006.

In other areas, the occurrence of SWB varied mainly tidally with time, although never precisely deterministic. For example, at 3000 m above the foot of the continental slope in the Rockall Channel Bonnin et al. (2006) observed in a 6-week record the largest sediment resuspension more or less at the turn of the tidal current for a time span of about 4 days only. In the highly tidally dominated Bay of Biscay van Haren (2006) established in a short, 2.5 days, but twice per second sampled record a 10% variation in the tidal timing of the otherwise steep and regular fronts followed by wildly varying 'waves'. This variation in timing of frontal arrival at the mooring had the same value as that leading to "intermittency" so often attributed to internal waves. It thus suggested intermittent internal tides at the source. As in other observations, all fronts were followed by turbulent but stratified waters, so that the bores' passage never led to a homogeneous bottom boundary layer, as was shown in 1-Hz temperature *T*-observations near the top of Atlantic Ocean's Great Meteor Seamount (van Haren, 2005). Recent, equally detailed ADCP-observations will be compared with *T*-observations in Section 3.2. Especially the dI-data will be used for comparison, because the current data are averaged over the beam spread, which yields somewhat different detailed results than *T*-data.

For example, the 2–55 m horizontal beam spread and the 1–2 Hz sampling allow the distinction of different arrival times t_i, $i=1,\ldots,4$, at different distances in the acoustic beams from sharp changes in dI-content associated with frontal non-linear and turbulent bores or 'waves'. The changes in dI are mainly due to variations in amounts of resuspended material carried by the near-bottom turbulence, and to some extent due to the fast variations in density stratification ('stratified turbulence'), as inferred from 1-Hz sampled thermistor string data above the ADCP. Such bores are observed to pass the mooring up to 80 m above the bottom having typical propagation phase speeds $c=0.15$–0.5 m s^{-1}, as determined from dI(t_i) (van Haren, 2007). Particle speeds in the immediate environment of a bore amount to $|u|_{env}=c\pm 0.05$ m s^{-1}, the equality being a necessary condition for kinematic instability. The maximum particle speeds amount $|u|_{max}=1.2$–$2c$. The dI-determined directions of up-, down- and alongslope processes are all within $\pm 10°$ of the ADCP's beam-spread averaged current (particle velocity) data.

3. Recent and revisited detailed observations

In this section newly analyzed historic and recent data are presented. The focus is on an observational view of different forms of "up-the-slope" propagating non-linear phenomena. The historic data are sampled at moderately high rates while the recent data at relatively high rates, which resolve the large

overturning turbulent scales O(1 m) vertically and O(10 m) horizontally, but certainly not the Kolmogorov or dissipation scales O(10^{-2} m). All data are raw data that are not filtered during post-processing but may be smoothed by instruments like an ADCP due to its vertical and horizontal averaging.

3.1. Vertical currents and upslope propagation

Although upslope propagation can be more precisely estimated using dI-information from the different beams of a fixed instrument, one has to refer to information from instrumentation at different moorings when attempting to follow the shoaling of an SWB. Such shoaling may affect the vertical currents, of which the large-scale ones are investigated here. Two FSC99 moorings are compared at 500 and 600 m halfway the 1% Shetland slope in the channel. On the former mooring, a bottom-fixed 300 kHz ADCP was mounted (80 m range with 1 m resolution, sampling interval once per 30 s) and on the latter a 75 kHz instrument that could freely spin at about 15 m above the bottom (500 m range with 10 m resolution, sampling interval once per 300 s).

Time series of w and dI on both ADCPs, some 9 km apart in cross-slope direction, show high-frequency large-amplitude excursions, appearing as spikes, with a maximum $|w| = 0.25$ m s^{-1} and typical values regularly >0.1 m s^{-1} (Figs. 4 and 5). These spikes have a duration of several minutes only, they are associated with T- and dI-frontal passages and they extend at least 80 m above the bottom, in some occasions several 100s of m, nearly the entire water column in the channel. As $|e| \ll |w|$ the vertical current is generally properly measured, values are well above noise level, and homogeneous across the beam spread over the sampling interval, even during large spikes like at day 111.79 (Fig. 4). Exception of $|e| = (0.1–1.0)|w|$ is the turbulent area associated with a near-bottom front, which however only appears in data that are sampled faster than the shortest buoyancy period $T_N \approx 120$ s, e.g., at day 112.42, ~465 m in Fig. 5.

The large vertical extent h_w of w, $h_w = O(0.1–0.9)H$ where H denotes the local water depth, shows no noticeable phase difference in w and suggests a 'low vertical mode' appearance. The initial frontal upward spike is followed by one or more series of down- and upward motions, which decrease in amplitude. This gives a line-appearance in w-data. Their periodicity with time is close to the local buoyancy period, either related to the thin layer stratification bordering the turbulent core or to the average large-scale background stratification.

The large-scale 75-kHz ADCP already demonstrates such high-frequency near-buoyancy waves. Upon the appearance of an upslope propagating bore the initial 'wave' periods (near days 111.8 and 112.3 in Fig. 4) are 1600–2000 s. This is comparable with $T_N = 1500 \pm 300$ s measured using thermistor string data just before the bore's arrival. However, these periods are much larger than the minimum buoyancy period

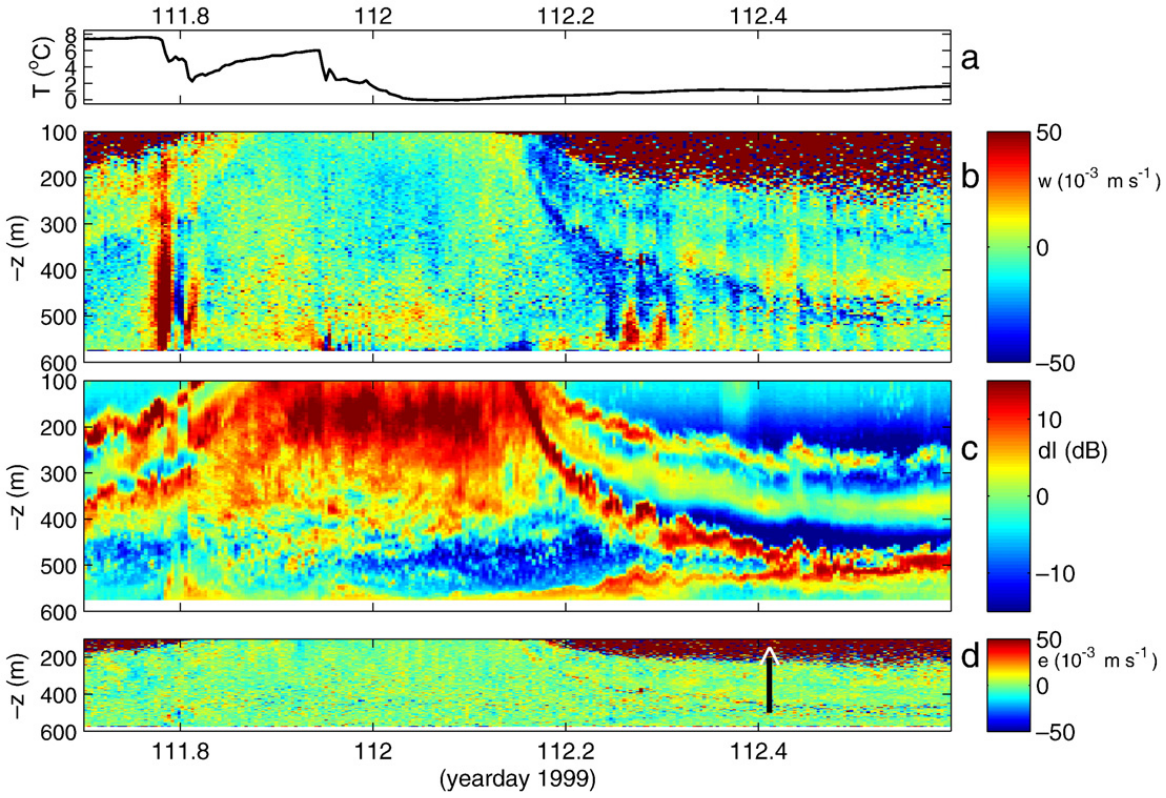

Fig. 4. Nearly 1-day time series of 300-s sampled 75-kHz ADCP data at 600 m water depth during FSC99 in April 1999. a. Temperature at 15 m above the bottom, b. depth–time plot of vertical current, c. relative echo intensity, and d. 'error' velocity, with the arrow indicating the time of frontal passage at 500 m water depth (Fig. 5). Brown colour in panels b. and d. indicates bad data due to lack of scatterers. These show a strong diurnal variation, with particles, mainly zooplankton, moving upward at sunset and downward at sunrise, as is clearly visible in dI-data (panel c.). (For interpretation of the references to colour in this figure legend, the reader is referred to the web version of this article.)

after the passage, which varies as a function of vertical scale height Δz: $T_N(\Delta z = 5\ \text{m}) = 300 \pm 30$ s compared with T_N ($\Delta z = 1$ m) $= 150 \pm 50$ s. Despite the relatively poor resolution, the 300-s sampled data do show high-frequency 'waves' emerge about 4 h after the largest bore passage (day 111.97 in Fig. 4). As was noted by Hosegood et al. (2004), near-buoyancy period waves occur 3.5–4 h after the largest frontal passage in the relatively better resolved 30-s sampled data from the 600-kHz ADCP (day 112.58 in Fig. 5). Overturning is noted in dI and *T* below these waves and thin vertical lining emerges in *w*. The shortest period is 120 s, which is equal to the local pycnocline's buoyancy period: a proper interface wave.

The low-mode *w*-appearance of the high-frequency internal waves, practically mode-1 with evanishing amplitudes near the bottom and in the weakly stratified near-surface layer, corresponds with the small phase differences observed in excursions of the thin layered stratification, resembled by dI and occasionally by *T*. The thin layers support the vertical current shear, which predominantly resides at low internal wave frequencies near the inertial frequency and at sub-inertial frequencies.

Despite the relatively short spatial separation between the two ADCPs, the bore's propagation is difficult to follow between the two moorings. For example, the bore passing at day 111.8 at 600 m (Fig. 4) is not at all found at 500 m (not shown). In general, the record from the latter site shows a four day periodicity in bore passages, while the former shows a few days of tidal periodicity as well. On the other hand, the waves passing at day ~112.25 at 600 m seem the same as those preceded by the largest bore passing at 500 m at day 112.4113 (Fig. 5). In this case, the wave is not noticed near the bottom at 600 m as the ADCP's temperature sensor shows no sudden decrease. Relating nevertheless the wave of depression at 112.245 in Fig. 4 to the bore in Fig. 5 we compute a propagation speed of ~0.65 m s^{-1}, which is close to the linear long wave phase speed estimate of $c = 0.64 \pm 0.18$ m s^{-1} (Hosegood et al., 2004). However, it is not well-established that the wave at 600 m becomes the bore at 500 m and a transfer from an apparent wave of depression to a wave of elevation is also not well-observed. One of the difficulties is the mode-2 appearance of the two waves as inferred from the two dI-interfaces approaching each other (Fig. 4c).

From the observations a first-order qualitative relation is obtained between local variation with time of *T*-data and the vertical advection inferred from *w*-data, so that $\partial T/\partial t$ has opposite sign of *w*, as in $\partial T/\partial t = -w\langle\partial T/\partial z\rangle$, where $\langle\rangle$ denotes a time mean.

3.2. Backwards breaking frontal waves

Temperature details of a 50 m backwards overturning front or breaking wave at 500 m near the top of Great Meteor Seamount have been discussed by van Haren (2005). Such frontal wave does not form closed-contoured boluses. The vigorous upslope propagating front sampled at 1-s and 1-m intervals is followed by increased stratification, much like noted in Section 3.1. This allows high-frequency waves of 10-times shorter periods than before the passage. Here, newly

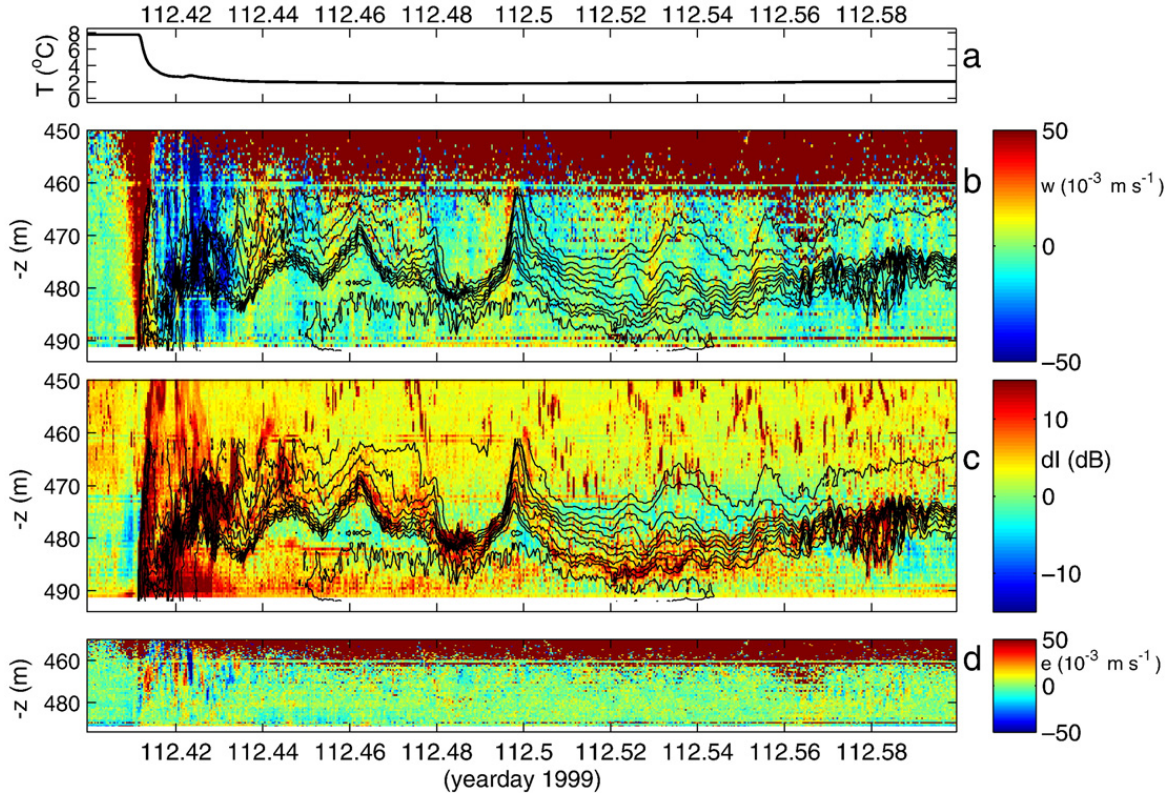

Fig. 5. As in Fig. 4 but for 4.8 hour time series of 30-s sampled 600-kHz ADCP data at 500 m water depth. This is the strongest frontal passage in this record while one tidal period earlier (day ~111.85) no front passed. The horizontal double lines are artificial reflections at thermistor string data loggers. The temperature record in panel a. is observed at 1.7 m above the bottom. The black contours in panels b. and c. represent isotherms every 0.5 °C between 2.0 and 7.5 °C. (For interpretation of the references to colour in this figure legend, the reader is referred to the web version of this article.)

obtained corresponding 2-s ADCP-data from the same area show more vertically smoothed ($\Delta z \approx 4$ m) but equally intense overturning echo intensity (Fig. 6). The four beams show different forms of passing fronts and overturning: at 40 m above the bottom they spread horizontally ~30 m and fronts are observed ~60 s (0.0007 day) apart in time.

Assuming the relative echo intensity is dominated by resuspended material, it is seen in Fig. 6 that it is swept up 40–50 m above the bottom by the strong vertical flow, more or less along the temperature front. About 150–200 s after the passage of the front, the material is depressed again and some of it is swept back to the front, apparently following a [turbulent] eddy that forms the core of the rotor ~10–20 m above the bottom. Several smaller scale and weaker rotors are seen, still some 10 m in vertical extent. As we shall see next, this sweeping up of material is not different from resuspension induced by boluses.

3.3. Trains of boluses

In September 2005, a NERC-initiative 'Slopemix' (coordinated by J.M. Huthnance) deployed several moorings in the FSC (FSC05), about 100 km closer to the Whyville Thomson Ridge 'WTR' than during FSC99. Compared with the 4-day periodicity in the 1999-data, the ADCP's *T*- and *w*-variability is highly tidal at this site. This may have to do with the approximation to a potential large source of internal tides, the WTR (Sherwin, 1991). However, the appearance of solibores during FSC05 is also different from the FSC99 site and not clearly tidally related. Unfortunately, the NIOZ-2 thermistor string failed and only ADCP-data are presented below.

The tidally dominant along-slope current *v* shows a semidiurnal periodicity that is different from the moments of appearance of vertically coherent spikes in *w* (Fig. 7; upper two panels). While the former is rather deterministic at the semidiurnal lunar periodicity, largest *w*-spikes pass more or less (to within $\pm 5\%$ of time) around the turn of the alongslope tidal current. This 10% variability in spike passing causes similar intermittence as the variability in frontal bore passage observed in the Bay of Biscay (van Haren, 2006). The most intense *w* does not occur during springtide: the example shown in the lower two panels of Fig. 7 is 2 days before neaptide. This is similar to some previous observations, e.g., in a fjord (Inall et al., 2000).

In further contrast with FSC99, the main frontal bore is replaced here by 3 boluses before a more or less regular train of waves at the near-bottom pycnocline emerges (Fig. 7). Nevertheless, a bolus shows the same characteristics as a solibore-front. Both are accompanied by large vertical up- and downgoing motions, with positive *w* preceding the bore or bolus. The low-mode appearance is reflected in the displacement of lines of constant temperature or of constant dI (cf., Fig. 7, lower

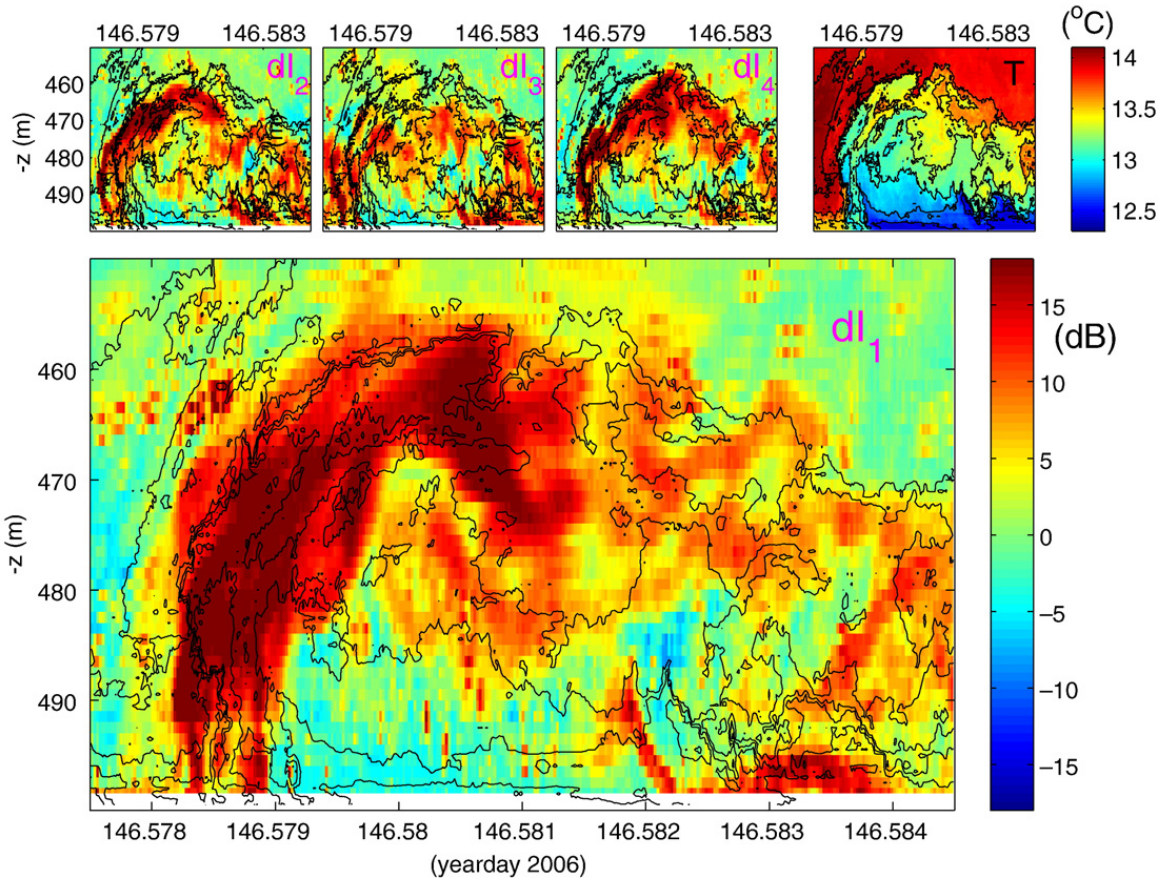

Fig. 6. Short 700-s record of relative echo intensity from 2-s 300-kHz ADCP relative echo intensity data compared with 1-s NIOZ-3 thermistor string data of large frontal passage above 550 m near the top of Great Meteor Seamount. All four beams are shown with 0.25 °C contours between 12.5 and 14.0 °C in black for reference. (For interpretation of the references to colour in this figure legend, the reader is referred to the web version of this article.)

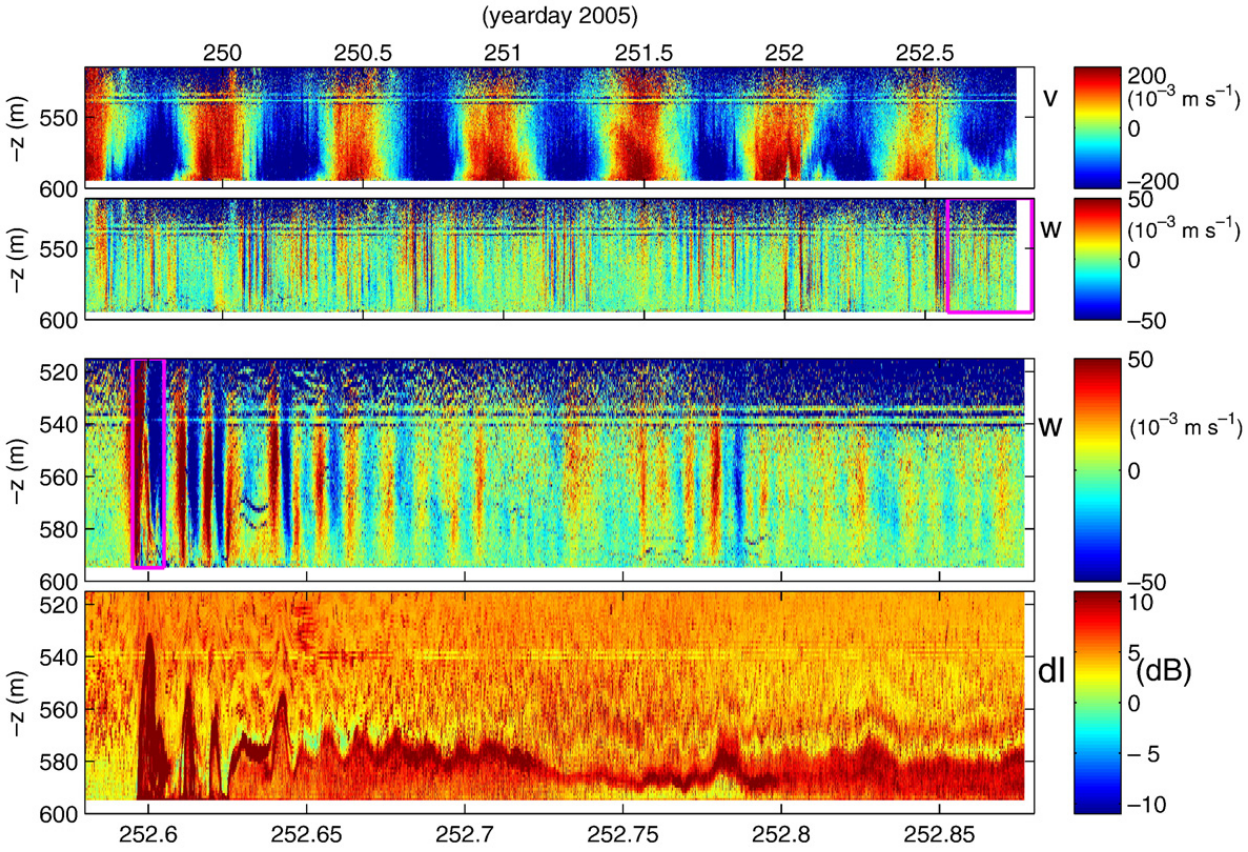

Fig. 7. Three day sample of 2-week deployment of 2-s sampling 300-kHz ADCP at 600 m in the FSC in September 2005. The site is 100 km to the southwest of FSC99. The upper two panels show the along-slope and the vertical current. The purple rectangle indicates the 7.2 hour period of the lower two panels, in which vertical current and relative echo intensity are shown. The purple rectangle in the *w*-panel indicates the 850 s period of Fig. 8. The horizontal lines around 540 m are reflections off the [non-functioning] thermistor string recorder. Above that depth regular periods of bad data (in dark-blue) occur due to lack of sufficient scatterers. (For interpretation of the references to colour in this figure legend, the reader is referred to the web version of this article.)

panel). Both the bore and the bolus are followed by enhanced stratification and their quasi-turbulent core is similar. This is also visible in the detail of the first bolus of a train (Fig. 8).

This bolus extends 60 m above the bottom and sweeps up an enormous amount of "material" along its frontal edge: the dI is 1000 times larger than its background value and is intruded into the bolus-core at its trailing edge. The core of turbulent motions is some 30 m above the bottom, at which sudden upslope motions of 0.75 m s^{-1} are reached. The core seems compact, with an apparent inner rotor of some 20 m high at time 252.601, but it is also somewhat open near the bottom at the trailing edge: a full and completely closed-contour bolus is not formed.

Above the bore's core or bolus streamlines are certainly not closed, as is inferred from the weakly visible "lines" in dI, and also in "bad data" in the current components. Streamlines are also observed in the occasional "double-hit" reflection off thermistor string sensors. These are ADCP's sidelobe reflections that provide an apparent double hit, presumably because of reflection at the frame or bottom.

4. Discussion

The transition of depression to elevation waves is not observed in near-bottom observations all ranging the lower part of the water column. But, such evidence has been clearly presented by Orr and Mignerey (2003) and indirectly by Bourgault et al. (2007) and there is no reason to assume that the present observations were all not initially [some kind of] internal solitary waves of depression. Upon approaching the bottom slope, the non-linearity of the wave becomes larger in the form of a steepening of the frontal face. This face is accompanied by a large upward motion, which confirms the modelling results by Vlasenko and Hutter (2002).

However, after the first front a distinct difference is found between the present (and previous) deep-ocean observations and the model results (that are depicted in Fig. 1c, right column). After the leading interface, the *model* shows a sequence of waves that do not obey the simple relationship $\partial T/\partial t = -w\partial T/\partial z$. Instead, the sign of w is wrong. In the present data, e.g. Fig. 5, w always has the opposite sign of the temperature time-derivative, no matter how small and rapid the near-buoyancy waves or bores are. As a result, the "large-scale" outercores of *observed* fronts and boluses more resemble a linear wave train of elevation propagating upslope.

The present experimental set-up was originally designed to estimate directly internal wave band momentum and heat fluxes (van Haren et al., 1994). Following several, not all unsuccessful attempts (e.g., Gemmrich and van Haren, 2002), it proved that especially heat fluxes are difficult to estimate

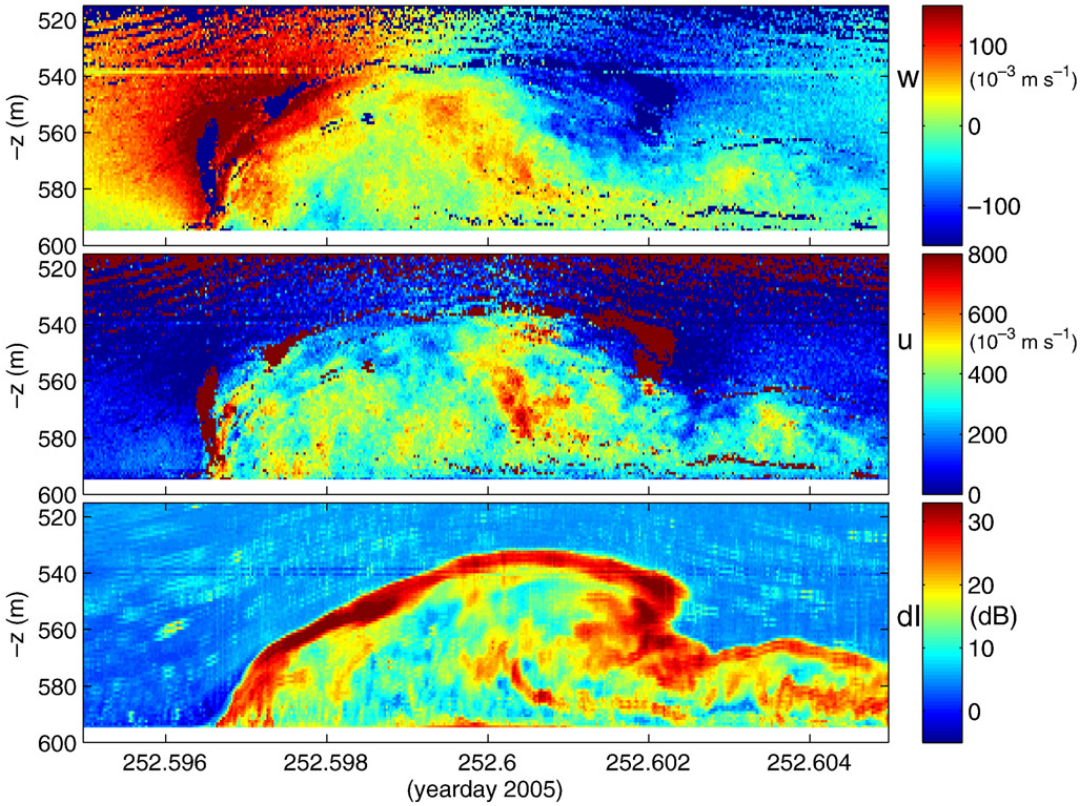

Fig. 8. Detailed depth–time series, ~850 s, or in horizontal scale ~400 m roughly estimated using propagation speed of 0.5 m s^{-1}, of a single bolus-bore from Fig. 7, comparing *w* with cross-slope *u* (only upslope values are coloured) and with relative echo intensity. The bad data (dark-blue in *w*, brown in *u*) may be used as tracer of streamlines following the passage of the bore, see also the dI-lines at the same depths. Note the different colour scales compared to Fig. 7. (For interpretation of the references to colour in this figure legend, the reader is referred to the web version of this article.)

using the present set-up, despite the very accurate modern temperature sensors. This difficulty in estimating heat fluxes has several reasons. Firstly, temperature sensors are heard by the ADCP (see double-hit reflectors in Fig. 8), which require substantial filtering of ADCP-data especially in the "under-sampled" ensembles that are stored at 0.5–1 Hz and contain 2–4 single pings. Secondly, the different scales of smoothing in ADCP and thermistor string cause different signals to be resolved (Figs. 6 and 8). The presented ~1 Hz sampling provides a new detailed view of inner-core quasi-turbulent motions, but their scales are too small to be resolved in ADCP-statistics that is homogeneous over its beam spread.

5. Conclusions

The high-sampling rate (~1 Hz) instrumentation of ADCP, and thermistor strings, resolving 1–3 m vertical scales over a range of 50–80 m has revealed the following characteristics of upslope propagating (soli)bores, boluses or waves of elevation in the deep ocean interior, which distinguish them from waves propagating obliquely up- and along sloping topography:

- SWB occur in very different shapes, as a turbulent frontal bore followed by waves, as boluses albeit not in single form but in trains of 3–10 waves, and as regular wave trains.
- They are found above a variety of slope conditions (from 'flat' ~<1% to steeper than 10%) at a variety of depths (verified between 100 and 3000 m).
- A unique source of generation seems not to exist, as both quasi-tidal and quasi-mesoscale atmospheric (or, perhaps, continental shelf wave) periodicities have been observed. So far, no spring-neap cycle in [frequency of] passages of SWB has been observed and spatial and temporal variabilities are much more intermittently, hence are much more unpredictable, than deterministic tides. However, without exception they seem to occur during minimal [alongslope] large-scale current.
- Spatial and temporal scales of important inner-core features are short, even compared to scales of passing the different beams of an ADCP. The buoyancy-scale waves are well-resolved by ADCP.
- The horizontal current and the relative echo intensity anomalies extend from ~4 (verified) up to 60 m above the bottom. However, the associated vertical currents can extend far beyond the range of the detailed instrumentation, at least 85 m above the bottom. They regularly extend into the upper half of the water column, more than 300 m above the bottom, thereby giving the impression of a 'low mode' internal wave.
- The detailed *w*-current structure consists of large-scale vertically coherent up and down motions occasionally exceeding 0.15 m s^{-1} ($|w/u| \sim 0.33$), it always starts the frontal passage with the upward motion and which is directly associated with the wave to first order. To second order, within the turbulent core, a mode-2 structure is observed towards the rear end of a single wave or bolus, with near-bottom upward motion under large-scale

downward motion. To higher order, quasi-turbulent, not well-resolved vertical motions are observed within the core of a single SWB.

- Horizontal currents are strictly directed upslope during the first frontal passage and attain velocities up to 0.75 m s^{-1}, in the present data. Like *w*, quasi-turbulent motions are observed in some detail within the core, which is most intense some 20–30 m above the bottom, which is about 40% of the total height of the SWB.
- The relative acoustic echo extends up to 30 dB above [1000 times larger than] the background level with the largest values along the outer rim of the single wave. This follows more or less the streamlines of the flow outside the turbulent core until it reaches the rear end where part of the resuspended material is sucked into the turbulent area.
- None of the SWB-forms, not even single boluses, generates completely closed large-scale 'outer' contours: they open near the bottom rear end.

6. Future development

The precise mechanisms of generation of different shapes of SWB are still unknown. Presently, the natural variability of occurrence is large in time and space while the spatial and temporal scales are relatively short. An ideally 3-dimensional mooring array would require resolution of 1 m vertically over a range of at least 100 m, and 10–100 m horizontally over a range of several 1000 m. So far, this seems impossible with moored instrumentation, especially at large depths. The resolution in time of 1 s is possible nowadays, but we require improved statistics. Future moored instrumentation should be running at 1 Hz for the duration of several months, preferably 1 year. The NIOZ-3 thermistor string development seems adequate for this purpose. Although one would like to observe direct estimates of vertical eddy fluxes, the development seems not suited for passing bores due to the too large spreading of the ADCP's beams with respect to the bores' scales.

Acknowledgments

I thank the crews of the R/V Pelagia and R/V Poseidon for deployment and recovery of the moorings. Theo Hillebrand and NIOZ-MTM prepared moorings and instrumentation. Fig. 2 was designed by NIOZ-MTM. PROCS and LOCO are supported by grants from NWO, The Netherlands organisation for the advancement of scientific research. SLOPEMIX is partially supported by NERC and NWO.

References

Bonnin, J., van Haren, H., Brummer, G.-J., Hosegood, P., 2006. Burst resuspension of seabed material at the foot of the continental slope in the Rockall Channel. Mar. Geol. 226, 167–184.

Bourgault, D., Blokhina, M.D., Mirshak, R., Kelley, D.E., 2007. Evolution of a shoaling internal solitary wavetrain. Geophys. Res. Lett. 34, L03601, doi:10.1029/2006GL028462.

Dauxois, T., Didier, A., Falcon, E., 2004. Observation of near-critical reflection of internal waves in a stably stratified fluid. Phys. Fluids 16, 1936–1940.

Gemmrich, J.R., van Haren, H., 2002. Internal wave band eddy fluxes in the bottom boundary layer above a continental slope. J. Mar. Res. 60, 227–253.

Grue, J., 2004. Internal wave fields analyzed by imaging velocimetry. In: Grue, J., Liu, P.L.-F., Pedersen, G.K. (Eds.), PIV and Water Waves. World Scientific Publishing, New Jersey, pp. 236–278.

Hosegood, P., Bonnin, J., van Haren, H., 2004. Solibore-induced sediment resuspension in the Faeroe–Shetland Channel. Geophys. Res. Lett. 31, L09301, doi:10.1029/2004GL019544.

Inall, M.E., Rippeth, T.P., Sherwin, T.J., 2000. Impact of nonlinear waves on the dissipation of internal tidal energy at a shelf break. J. Geophys. Res. 105, 8687–8705.

Ivey, G.N., Nokes, R.I., 1989. Vertical mixing due to breaking of critical internal waves on sloping boundaries. J. Fluid Mech. 204, 479–500.

Klymak, J.M., Moum, J.N., 2003. Internal solitary waves of elevation advancing on a shoaling shelf. Geophys. Res. Lett. 30 (20), 2045, doi:10.1029/2003GL017706.

LaFond, E.C., 1966. Internal waves. In: Fairbridge, R.W. (Ed.), The Encyclopedia of Oceanography. Reinhold Publishing Corporation, New York, pp. 402–408.

Merckelbach, L.M., 2006. A model for high-frequency acoustic Doppler current profiler backscatter from suspended sediment in strong currents. Cont. Shelf Res. 26, 1316–1335.

Moum, J.N., Farmer, D.M., Smyth, W.D., Armi, L., Vagle, S., 2003. Structure and generation of turbulence at interfaces strained by internal solitary waves propagating shoreward over the continental shelf. J. Phys. Oceanogr. 33, 2093–2112.

Orr, M.H., Mignerey, P.C., 2003. Nonlinear waves in the South China Sea: observation of the conversion of depression internal waves to elevation internal waves. J. Geophys. Res. 108 (C3), 3064, doi:10.1029/2001JC001163.

Sherwin, T.J., 1991. Evidence of a deep internal tide in the Faeroe–Shetland Channel. In: Parker, B.B. (Ed.), Tidal Hydrodynamics. Wiley, New York, pp. 469–488.

van Haren, H., 2005. Details of stratification in a sloping bottom boundary layer of Great Meteor Seamount. Geophys. Res. Lett. 32, L07606, doi:10.1029/2004GL02298.

van Haren, H., 2006. Nonlinear motions at the internal tide source. Geophys. Res. Lett. 33, L11605, doi:10.1029/2006GL025851.

van Haren, H., 2007. Echo intensity data as a directional antenna for observing processes above sloping ocean bottoms. Ocean Dyn. 57, 135–149.

van Haren, H., Oakey, N., Garrett, C., 1994. Measurements of internal wave band eddy fluxes above a sloping bottom. J. Mar. Res. 52, 909–946.

Venayagamoorthy, S.K., Fringer, O.B., 2005. Nonhydrostatic and nonlinear contributions to the energy flux budget in nonlinear internal waves. Geophys. Res. Lett. 32, L15603, doi:10.1029/2005GL023432.

Vlasenko, V., Hutter, K., 2002. Numerical experiments on the breaking of solitary internal waves over a slope-shelf topography. J. Phys. Oceanogr. 32, 1779–1793.

Wallace, B.C., Wilkinson, D.L., 1988. Run-up of internal waves on a gentle slope in a two-layered system. J. Fluid Mech. 191, 419–442.